Applied Energy 103 (2013) 155–164

Contents lists available at SciVerse ScienceDirect

Applied Energy

journal homepage: www.elsevier.com/locate/apenergy

Optimum capacity determination of stand-alone hybrid generation system considering cost and reliability

Hung-Cheng Chen *

Department of Electrical Engineering, National Chin-Yi University of Technology, 57, Sec. 2, Chungshan Rd., Taiping Dist., Taichung 41107, Taiwan

HIGHLIGHTS

- This paper presents a methodology for the installation capacity optimization.
- Hybrid generation system is optimized by application of adaptive genetic algorithm.
- A cost investigation is made under various conditions and component characteristics.
- The optimization scheme is validated to meet the annual power load demand.

ARTICLE INFO

Article history:
Received 15 May 2012
Received in revised form 15 August 2012
Accepted 11 September 2012
Available online 8 October 2012

Keywords:
Hybrid generation system
Installation capacity optimization
Adaptive genetic algorithm
Loss of load probability

ABSTRACT

The aim of this work is to present an optimization methodology for the installation capacity of a stand-alone hybrid generation system, taking into consideration the cost and reliability. Firstly, on the basis of derived steady state models of a wind generator (WG), a photovoltaic array (PV), a battery and an inverter, the hybrid generation system is modeled for the purpose of capacity optimization. Secondly, the power system is analyzed for determining both the system structure and the operation control strategy. Thirdly, according to hourly weather database of wind speed, temperature and solar irradiation, annual power generation capacity is estimated for the system match design in order that an annual power load demand can be met.

The capacity determination of a hybrid generation system becomes complicated as a result of the uncertainty in the renewable energy together with load demand and the nonlinearity of system components. Aimed at the power system reliability and the cost minimization, the capacity of a hybrid generation system is optimized by application of an adaptive genetic algorithm (AGA) to individual power generation units. A total cost investigation is made under various conditions, such as wind generator power curves, battery discharge depth and the loss of load probability (LOLP). At the end of this work, the capacity of a hybrid generation system is optimized at two installation sites, namely the offshore Orchid Island and Wuchi in Taiwan. The optimization scheme is validated to optimize power capacities of a photovoltaic array, a battery and a wind turbine generator with a relative computational simplicity.

1. Introduction

The demand for renewable energy sources continues to grow in such a rapid pace that solar/wind hybrid generation systems have received plenty of attention due to the advantages of reliability and low cost [1–5]. However, a single photovoltaic system or wind power generation system is very unlikely to provide a stable electricity supply due to low energy density and high randomness. For this sake, an energy storage device is introduced into a power system as an auxiliary unit to improve the electricity supply quality at an elevated cost [6–9]. It becomes an immediate concern to find a solution to the capacity optimization of a hybrid generation system while keeping the cost down [10–13]. The key is to find an appropriate approach to reach a matched system such that wind/solar energy sources can be used to the greatest extent.

A number of research tasks had been done in dealing with the design and the sizing of hybrid systems [14–17]. In [14], based on energy generation simulation for various numbers of PVs and batteries, using suitable models for the system devices, a sizing method of stand-alone PV systems has been presented. The selection of the numbers of PVs and batteries ensures that reliability indices such as the loss of load hours (LOLH), the lost energy and the system cost are satisfied. Similarly in [15], a Markov chain model is used for the solar radiation. The numbers of PVs and batteries are selected according to the intended System Performance

* Tel.: +886 423924505; fax: +886 423924419.
E-mail address: hcchen@ncut.edu.tw

0306-2619/$ - see front matter © 2012 Elsevier Ltd. All rights reserved.
http://dx.doi.org/10.1016/j.apenergy.2012.09.022

Level (SPL) requirement, which is defined as the number of days that the load cannot be met and expressed in terms of probability. In [16], the generation capacity is determined to best match the power demand by minimizing the difference between generation and load over a 24-h period based on the available hourly average data of wind speed, irradiation and the power demand. The iterative procedure is adopted for selecting the wind turbine size and the number of PV panels needed for a stand-alone system to meet a specific load. An alternative methodology for the optimal sizing of stand-alone PV/WG systems has been proposed in [17]. The purpose is to suggest the optimal number and type of units, among a list of commercially available system devices, to ensure that the 20-year round total system cost is minimized subject to the constraint that the load energy requirements are completely covered. A simple genetic algorithm is then used to minimize the cost function.

A disadvantage that all the aforementioned works have in common is that the system design characteristics, such as the wind generator power curve, the installation height of wind turbine and the state of charge (SOC) of a battery, are not taken into account, when a hybrid generation system is designed. Both the power production and installation cost are found highly affected by such characteristics. A point worthy of mention is that the consumer power demand is estimated as an hourly average over a 24 h period, that is, it does not truly reflect the variation of practical power requirement over 8760 h a year. An objective function is optimized by means of either a linear programming technique or a simple genetic algorithm, giving rise to a local optimal solution and a higher computational load.

Accordingly, this work presents an alternative to previous methodologies for the capacity optimization of a wind/solar stand alone hybrid generation system. As the first step, the system is configured and an appropriate operation strategy must be determined, and then the installation capacity is optimized in consideration of annual power demand, wind speed, temperature and solar irradiation in a field. The quantities required to be optimized in a generation system include the capacities of photovoltaic array, battery and the capacity as well as the types of wind power generators. The total capital cost is treated as an optimization objective, while other quantities are as constrained conditions, namely, decision variables, system operation process and power supply reliability. The capacity optimization of a hybrid generation system turns highly complicated, in the course of the objective function minimization, due to the uncertainty in the renewable energy together with load demand and the nonlinearity of system components. For this sake, underlain by an adaptive genetic algorithm (AGA) proposed by the author [18], individual power capacity is optimized in an entire system. The minimization of the cost (objective) function is implemented employing the AGA approach. It has been shown to be highly applicable to cases of large nonlinear systems, where locating the global optimum is a difficult task. Due to the improved adaptability, AGA exhibits the ability to attain the global optimum with relative computational simplicity. Thus, given the number of existent nonlinearities in various structures of a hybrid generation system, AGA appears to be a useful approach.

2. Hybrid generation system modeling

2.1. Photovoltaic system

Consisting of a large number of jointly connected solar cells, a PV module is a building block in a photovoltaic system of any kind. There have been a number of solar cell models developed, among which the one diode electrical equivalent circuit, as shown in Fig. 1a, is the most commonly used one for a cell, or module, based

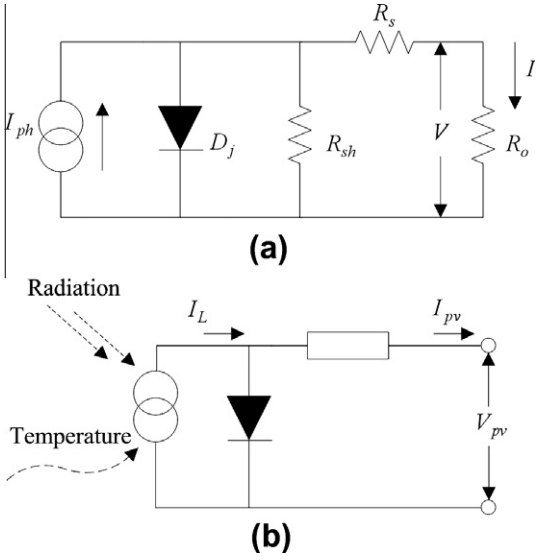

Fig. 1. PV module (a) equivalent circuit and (b) simplified version.

analysis. It is composed of a diode, a series resistance and a parallel resistance and a current source that generates the photo-current, a function of the incident solar cell radiation and temperature [19–21]. The diode represents the p–n junction of a solar cell, and the temperature dependence of the diode saturation current and constant diode ideality factor are taken into account in the model. Modeled as a series resistance R_s, a voltage loss on the way to the external contacts is observed at practical solar cells. Furthermore leakage currents are described by a parallel resistance R_{sh}. However, the rather low series resistance and the rather high parallel resistance [21] can be respectively approximated as short circuit and open circuit, leading to a simplified version of the solar cell model as illustrated in Fig. 1b.

In a PV module, the current and the voltage equations are respectively expressed as

$$I_{pv}(t) = I_{sc}\left\{1 - C_1\left[\exp\left(\frac{V_{mp}}{C_2 V_{oc}}\right) - 1\right]\right\} + \left(\frac{E_{tt}(t)}{E_{st}}\right)[\alpha(T_a(t) + 0.002E_{tt}(t) + 1)] - I_{mp} \quad (1)$$

and

$$V_{pv}(t) = V_{mp}\left[1 + 0.0539\log\left(\frac{E_{tt}(t)}{E_{st}}\right)\right] + \beta(T_a(t) + 0.02E_{tt}(t)) \quad (2)$$

$$C_1 = \left(1 - \frac{I_{mp}}{I_{sc}}\right)\exp\left[\frac{-V_{mp}}{C_2 V_{oc}}\right] \quad (3)$$

$$C_2 = \frac{\frac{V_{mp}}{V_{oc}} - 1}{\ln\left(1 - \frac{I_{mp}}{I_{sc}}\right)} \quad (4)$$

The power equation is expressed as

$$P_{pv}(t) = V_{pv}(t)I_{pv}(t) \quad (5)$$

where I_{sc} represents the short circuit current at 25 °C and 1 kW/m^2, V_{oc} the open circuit voltage at 25 °C and 1 kW/m^2, I_{mp} the maximum power current, V_{mp} the maximum power voltage, E_{st} a solar radiation reference (1 kW/m^2), $E_{tt}(t)$ the solar radiation at any time instant t, T_a (t) the ambient temperature at any time instant t, α the short circuit current temperature coefficient, and β the open circuit voltage temperature coefficient.

A GEPVp-200W PV module is adopted in this work with parameters tabulated in Table 1. The power capacity of such PV module

Table 1
Specifications of a GEPVp-200 W PV module.

Typical performance characteristics		
Peak power (Wp)	Watts	200
Max. power Voltage (Vmp)	Volts	26.3
Max. power current (Imp)	Amps	7.6
Open circuit voltage (Voc)	Volts	32.9
Short circuit current (Isc)	Amps	8.1
Short circuit temp. coefficient	mA/°C	5.6
Open circuit voltage coefficient	V/°C	−0.12
Max. power temp. coefficient	%/°C	−0.5
Max. series fuse	Amps	15
Normal operating cell temperature	°C	45

can be evaluated according to the solar irradiation and the ambient temperature at an installation site.

The accuracy of the electricity model is validated using PV manufacture datasheets. PV manufactures generally only provide experimental data with reference to standard test condition (STC) and the nominal conditions. In order to validate the *I–V* and *P–V* output characteristics of PV electricity model at the so-called STC, the cell temperature is fixed at 25°, the solar irradiance is given by 1 kW/m^2, and the operating voltage increases from 0 V to 20 V at 0.1 V steps. Compared with the characteristic curves provided by manufacture, it is validated that the model has a good degree of match with the experimental data of PV manufacture datasheets in the standard test conditions.

2.2. Wind generator

Given a wind speed, the output power of a wind generator (WG) is found according to a power-speed curve at the installation site. With a hub height of 64.7 m, an output frequency of 60 Hz and an output voltage of 690 V, four types of generators, Enercon E40, Dewind D4-48, Nordex N43 and Vestas V42 as shown in Fig. 2, all rated at 600 KW, are chosen as the candidates for the best capacity optimization.

As a rule, the wind speed information available to the public is measured at the height of an anemometer, rather than at the installation height. Hence, the reference wind speed at a reference height must be converted into that of interest by

$$v_1 = v_2\left(\frac{h_1}{h_2}\right)^{\gamma} \tag{6}$$

where v_1 symbolizes the wind speed at the installation height h_1, v_2 the wind speed at reference height h_2, and γ the power-law exponent (1/7 for open land).

For the purpose of power analysis, a set of power-speed data is fitted into an 8th-order polynomial $P_{wg}(v)$, expressed as

$$P_{wg}(v) = \begin{cases} 0 & (v < v_{ci}) \\ P'_{wg}(v) & (v_{ci} \leqslant v \leqslant v_{co}) \\ 0 & (v > v_{co}) \end{cases} \tag{7}$$

where v_{ci} denotes the cut-in wind speed, v_{co} the cut-out wind speed, and $P'_{wg}(v)$ an 8th-order polynomial for a WG power-speed curve fitting.

The output power and speed data of a wind generator according the power-speed curve provided by manufacture are fitted into a polynomial function. The accuracy of the fitted power-speed curve can be validated by comparing the function values with the power-speed curve. The wind speed information available to the public is measured at the height of an anemometer, rather than at the installation height. Hence, the reference wind speed at a reference height must be converted into that of interest.

2.3. Battery

In a Kinetic model [22], a battery is modeled as a voltage source E_B, dependent on the state of charge, in series with an internal resistor R_o, as illustrated in Fig. 3, which symbolizes the charge resistance R_{ch} in a charge state, while symbolizes the discharge resistance R_{dch} in a discharge state.

Accordingly, the terminal voltage V_B of the battery is given as

$$V_B = E_B - I_B R_o \tag{8}$$

where I_B represents the output current.

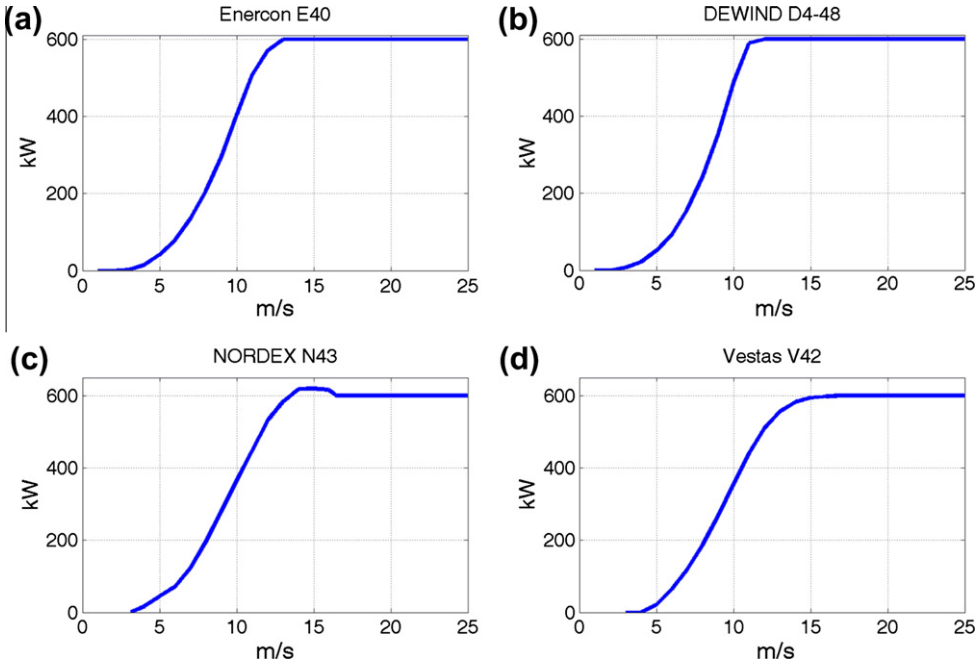

Fig. 2. WG power-speed curves (a) Enercon E40, (b) Dewind D4-48, (c) Nordex N43 and (d) Vestas V42.

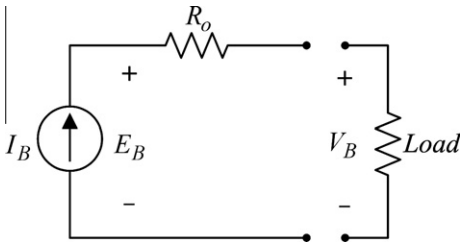

Fig. 3. Equivalent circuit of battery.

Adopted in this work, a CSB-manufactured valve regulated lead-acid battery TPL121500 has two fitted curves for the terminal voltages in the charge and discharge state respectively, which are expressed in function of state of charge as

$$V_{Bch} = 12 + 0.888\frac{\mathrm{SOC}(t)}{\mathrm{SOC}_{\max}} \tag{9}$$

$$V_{Bdch} = 11.556 + 0.744\frac{\mathrm{SOC}(t)}{\mathrm{SOC}_{\max}} \tag{10}$$

where SOC(t) signifies the state of charge at any time instant t, and SOC_{max} the maximum value of SOC.

The temperature dependence of V_B is given by

$$V_B = V_{B0}[1.0 - 0.001(T - 25)] \tag{11}$$

where V_{B0} represents the terminal voltage of a battery at 25 °C, and T the ambient temperature.

The amount of charge $Q_B(t+1)$ released/supplied by a battery at a given time instant is related to $Q_B(t)$ at the previous instant by

$$Q_B(t+1) = Q_B(t)(1 - D_s) + K(V_B I_B - R_0 I_B^2) \tag{12}$$

where D_s and K denote self-discharge rate and charge/discharge efficiency of a battery, respectively. As a function of the battery charge current, $0.9 \leqslant K \leqslant 1$ in a charge state, while $0.65 \leqslant K \leqslant 0.85$ in a discharge state.

A battery is not permitted to go beyond its ratings in either a charge or a discharge state. In case the terminal current $I_B > I_{Bdch\max}$ in a discharge state, set $I_B = I_{Bdch\max}$, and the maximum amount of discharge is then equal to $I_{Bdch\max}\,\Delta t$; while $I_B = I_{Bch\max}$ provided that $I_B > I_{Bch\max}$ in a charge state, and the maximum amount of charge is $I_{Bch\max}\,\Delta t$. where $I_{Bch\max}(t)$ and $I_{Bdch\max}(t)$ represent the maximum charge and discharge currents, respectively.

The battery is modeled in a simple Kinetic model. The internal resistance is an essential specification in datasheet, which stands for electrolyte, connection resistances and charge transfer resistance. The terminal voltage depending on the state of charge are approximately fitted using curve fitting technique from characteristic curves provided by battery manufactures. The battery model is east to implemented and validated according to the manufacture datasheets.

2.4. Inverter

In a hybrid generation system, a high conversion efficiency inverter is found critical, in particular in a light load condition. The input power P_{inv_in} applied to an inverter is related to the output power P_{inv_out} by

$$P_{inv\_out} = P_{inv\_in} \times \eta_{inv} \tag{13}$$

where η_{inv} represents the efficiency of an inverter.

The input DC current is given as

$$I_{inv} = \frac{I_{ac} \times V_{ac}}{V_{dc} \times \eta_{inv}} \tag{14}$$

where I_{inv} denotes the input current of an inverter, I_{ac} the AC side load current, V_a the AC side voltage, and V_{dc} the DC side voltage.

3. Optimum capacity determination using AGA

Proven more efficient than conventional algorithms, genetic algorithms are developed as a random search approach to locate the global optimum. However, in consideration of distinct nature of search problems, a simple GA is not expected to find the global optimum as intended [23]. In an effort to handle a local convergence problem, an AGA, a prior work of author [18], is adopted to search all the power units across the entire system, that is, wind power generators, photovoltaic arrays and batteries, for the capacity optimums thereof.

3.1. Hybrid generation system structure and operation control strategy

Composed of photovoltaic arrays, wind generators, batteries, inverters, and a diesel generator, the considered stand-alone hybrid generation system, as configured in Fig. 4, is dealt with for capacity optimization in this work. As a auxiliary power source, the diesel generator is operated to delivers power to load in bad weather conditions that disables the hybrid generation system.

The optimized capacity is found not merely related to the selections of power units, but also related to the operation control strategy employed. Detailed in Fig. 5 is an operation control strategy, according to which an intended amount of electricity is provided at any time by the first use of renewable energy sources with a quality assured electricity supply.

The loss of load probability (LOLP), as suggested in [24], is adopted as a measure of a system reliability, defined as

$$\mathrm{LOLP} = \frac{\mathrm{LOLH}}{T} \tag{15}$$

where T represents a one-year period (8760 h), LOLH the loss of load hour over T, defined as

$$\mathrm{LOLH} = \sum_{t=1}^{T} Z(t) \tag{16}$$

where

$$Z(t) = \begin{cases} 1 & \text{When the generator starts} \\ 0 & \text{When the generator stops} \end{cases} \tag{17}$$

A zero LOLP indicates a 100% reliability, stating that a hybrid generation system can fully fulfill the load demand all the time, while an LOLP of 1 indicates a poor reliability, that is, the load demand is unlikely to be met any time.

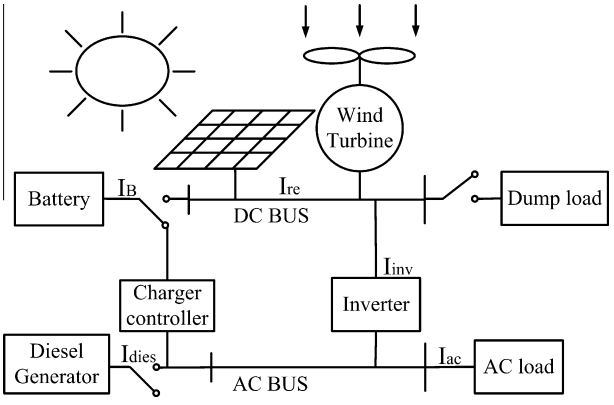

Fig. 4. Hybrid generation system structure.

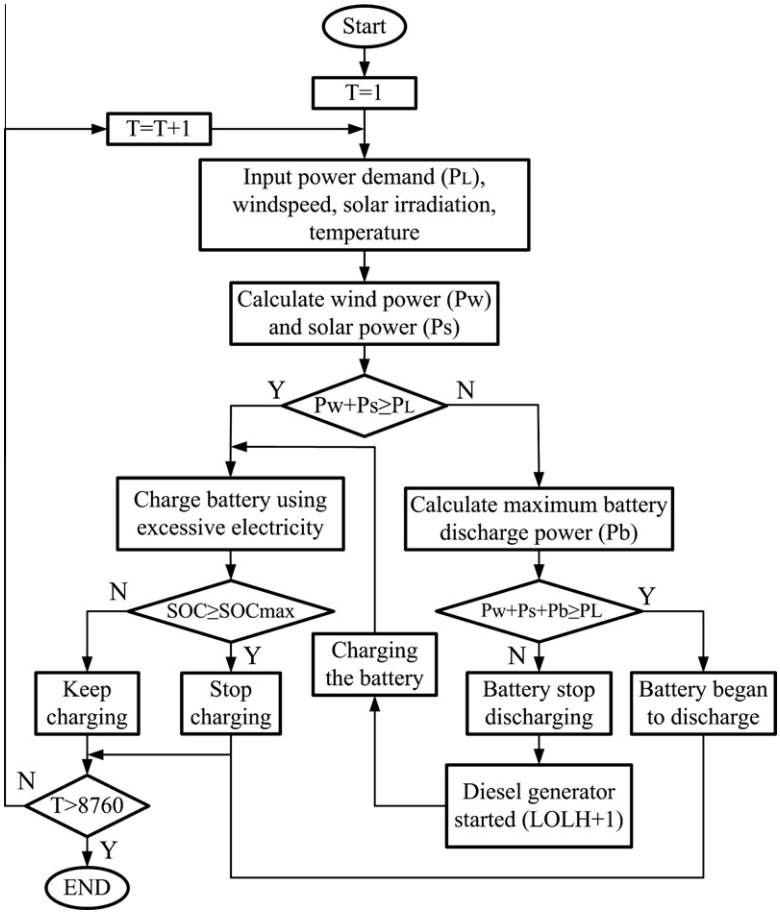

Fig. 5. Operation control strategy for the proposed hybrid generation system.

The value of LOLP, ranging between 0 and 1 in most cases, is determined by a tradeoff between the installation cost and the system reliability. When the total power capacity of the renewable energy sources and the battery are found not able to meet the load demand, the diesel generator is activated and gets the battery charged. In this case, an elevated value of LOLP by 1 represents the amount of time that the diesel generator operates.

In this presented strategy, there are three operation modes for AC side current as follows.

(1) In case the renewable energy sources can meet the load demand, an excessive amount of electricity is delivered to the battery, that is

$$I_{ac} = I_{inv} \times \eta_{inv} \times (V_{dc}/V_{ac}) \tag{18}$$

$$I_{inv} = I_{re} - I_{Bch} \tag{19}$$

where I_{Bch} denotes the charge current through the battery, formulated as

$$I_{Bch} = \min[I_{re} - I_{inv}, I_{Bch\max}] \tag{20}$$

(2) In case the load demand can be fulfilled only when both the renewable energy sources and the battery are activated, then the battery is discharged at a discharging current I_{Bdch} as given in Eq. (23). Respective current are related as

$$I_{ac} = I_{inv} \times \eta_{inv} \times (V_{dc}/V_{ac}) \tag{21}$$

$$I_{inv} = I_{re} + I_{Bdch} \tag{22}$$

$$I_{Bdch} = \min[I_{Bdch\max}, I_{inv} - I_{re}] \tag{23}$$

(3) In case a combination of the renewable energy sources and the battery is unlikely to meet the load demand, the diesel generator is then activated and simultaneously charges the battery as well. Respective current are related by

$$I_{ac} = I'_{inv} + I_{dies1} \tag{24}$$

where

$$I'_{inv} = I_{re} \times \eta_{inv} \times (V_{dc}/V_{ac}) \tag{25}$$

$$I_{dies1} = \min[I_{dies\max},\ I_{ac} - I'_{inv}] \tag{26}$$

$$I_{Bch} = \min\ [I_{dies\max} - I_{dies1},\ I_{Bch\max}] \tag{27}$$

$$I_{dies} = I_{dies1} + I_{Bch} \tag{28}$$

where I_{dies} and $I_{dies\max}$ denote the output current and the rated output current of the diesel generator, respectively.

3.2. Decision variables

In a hybrid generation system, the decision variables refer to the capacities (numbers) of respective system components. In this work, it is represented as a vector

$$X = [X_w, X_s, X_b] \tag{29}$$

where X_w represents the number of wind generators, X_s the number of parallel connected photovoltaic arrays, and X_b the number of batteries wired in parallel.

The installation capacity of a hybrid generation system is optimized according to the decision variables as well as the operation control strategy chosen.

3.3. Objective function

An objective function is defined as a function of the decision variables selected. In the first place, the cost must go down in a hybrid generation system design scheme, that is, a minimum number of wind generators, photovoltaic arrays and batteries are employed while meeting the power load demand. Hence, the objective function in this work is defined as the total installation cost

$$C = P_w \times X_w + P_s \times X_s + P_b \times X_b \tag{30}$$

where P_w, P_s and P_b represent the unit prices of a wind generator, a photovoltaic array and a battery, respectively.

3.4. Constraint conditions

Constraint conditions refer to the ranges of decision variables being considered according to the nature of a generation system. The constraints imposed on the stand-alone hybrid generation system include decision variables, supply and demand balance in power system operation and system reliability, which are detailed respectively as follows. They are categorized into three classes.

(1) On the decision variables
As part of a power system, the battery current must satisfy the condition

$$SOC_{\min}(t) \leqslant X_b \times I_B \leqslant SOC_{\max}(t) \tag{31}$$

(2) On the system operation
An adequate level of AC current must be supplied by the hybrid generation system to the load, that is

$$I_{ac} = I_{\text{load}} \tag{32}$$

where I_{load} denotes the load current.

(3) On the system reliability
The operation control strategy adopted in this work makes the first use of renewable energy sources while ensuring a reliable power system operation. The LOLP is defined as a measure of system reliability with an upper bound

$$\text{LOLP}\ (X_w,\ X_s,\ X_b) \leqslant r \tag{33}$$

where r represents the maximum value of LOLP accepted.

3.5. Adaptive genetic algorithm

The detailed crossover and mutation operations of the AGA used in this paper are summarized as follows [18]:

(1) Crossover operation

Crossover used here is single-point method. Setting two randomly selected chromosomes at i generation as $X_k^i = [x_{k1}^i, x_{k2}^i, x_{k3}^i]$ and $X_l^i = [x_{l1}^i, x_{l2}^i, x_{l3}^i]$, the genetic values at the crossover point of these two chromosomes are x_{kj}^i and x_{lj}^i respectively. Two new chromosomes would be created after the crossover operation. The genetic values before and after crossover point remain the same, while the genetic value of the crossover point is

$$\begin{aligned} x_{kj}^{i'} &= r_c x_{kj}^i + (1 - r_c) x_{lj}^i \\ x_{lj}^{i'} &= r_c x_{lj}^i + (1 - r_c) x_{kj}^i \end{aligned} \tag{34}$$

where r_c is the randomly generated constant between 0 and 1. Crossover operation is the major technique to generate new individual in genetic algorithm, and the crossover rate would generally pick the larger value. However if the crossover rate is picked too large, it might damage the good pattern of the population; if the value is too small, then the speed to generate the new individual is too slow. Furthermore, the less diversity of the population is the major cause for the instability and premature of GA. One should take measures before the diversity of population is getting poor. Therefore this paper puts forward the adaptive method which took the diversity of the population as the controlled variable and also adjusted the individual crossover rate based on the fitness value of itself. The adaptive crossover rate of an individual is defined as

$$p_c = \begin{cases} \frac{k_c}{(f_{\max} - f_{avg})/f_{avg}} + p_{c1}\, e^{-\frac{c}{\tau_c}(f_c - f_{avg})} & f_c \geqslant f_{avg} \\ \frac{k_c}{(f_{\max} - f_{avg})/f_{avg}} + p_{c1} & f_c < f_{avg} \end{cases} \tag{35}$$

where

$$\tau_c = \frac{f_{\max} - f_{avg}}{\ell n(p_{c1}/p_{c2})}$$

$f_{\max}$ is the maximal fitness value of the present population. f_{avg} is the average fitness value of the present population. f_c is the larger fitness value of the two individual who would intersect; k_c, p_{c1} and p_{c2} are the crossover coefficients, $p_{c1} > p_{c2}$ and they are the constants between 0 and 1, c the crossover amplitude coefficient.

In Eq. (35), the denominator $(f_{\max} - f_{avg})/f_{avg}$ of the first term at the right side of the equation is an index to represent the diversity of the population during the computation process of genetic algorithm, which is called dispersion degree. Therefore the adaptive quantity which would vary with dispersion degree is added to the first term. The smaller dispersion degree represents that the individuals' fitness values within the population are moving forward in harmony or the population has converged to a local optimal solution, then the first term would rise to increase the crossover rate. On the contrary, the larger dispersion degree represents that the population is scattered in the solution space, the value of the first term drops and then the crossover rate decreases. The second adaptive quantity which would vary with the fitness is added to the second term at the right side in Eq. (35). The individual would be assigned a larger crossover rate p_{c1} when its fitness is worse than average (i.e. $f_c < f_{avg}$). If the fitness of the individual is better than average (i.e. $f_c \geqslant f_{avg}$), this individual would be assigned a smaller crossover rate which is exponentially decreased with the fitness beyond the average. In Eq. (35) we can observe that the crossover rate becomes smaller when the fitness value approaches the maximal fitness. When the fitness is equal to the maximal fitness, the crossover rate is p_{c2} rather than 0. The individual with the maximal fitness is uncertain of the global optimal solution. By using the adaptive crossover rate in Eq. (35), the fine individuals also have the chance to undergo the crossover operation, so that they would not get stuck at a local optimum.

(2) Mutation operation

Mutation used here is non-uniform method. Set the mutation operation individual as $X_k^i = [x_{k1}^i,\ x_{k2}^i,\ x_{k3}^i]$, after the mutation operation, the genetic value of the individual which is not mutated remains the same, while the gene $x_{k_j}^{i'}$ on the mutated one is

$$x_{k_j}^{i'} = \begin{cases} x_{k_j}^i + \delta(i,\ x_{j\max} - x_{k_j}^i) & r_m \geqslant 0.5 \\ x_{k_j}^i - \delta(i,\ x_{k_j}^i - x_{j\min}) & r_m < 0.5 \end{cases} \tag{36}$$

where r_m is a random number between 0 and 1. $\delta(i, y)$ represents a random number within the range of [0,y], which is varying with evaluation generation. The expression of $\delta(i, y)$ is

$$\delta(i, y) = y\left(1 - r^{\left(1 - \frac{i}{G}\right)^b}\right) \tag{37}$$

where r is a random number between 0 and 1. i is the present evolution generation. G is the set maximal evolution generation. b is the

coefficient that determines the dependency of stochastic disturbance on evolution generation i, which is generally determined by the experience, one would pick $b = 2$ in this research. Mutation rate has an important effect on the parametric optimization. If it is too large, the optimization procedure would not converge; if it is too small, then the GA might lead to prematurity. In the same way, the variation of diversity of the population is also the major cause for prematurity of GA. One should take measures before the diversity of population is getting poor. Therefore this paper puts forward the adaptive method which took the diversity of the population as the controlled variable and also adjusted the individual mutation rate based on the fitness value of itself. The adaptive mutation rate of an individual is defined as

$$p_m = \begin{cases} \frac{k_m}{(f_{\max} - f_{avg})/f_{avg}} + p_{m1}\, e^{-\frac{m}{\tau_m}(f_m - f_{avg})} & f_m \geqslant f_{avg} \\ \frac{k_m}{(f_{\max} - f_{avg})/f_{avg}} + p_{m1} & f_m < f_{avg} \end{cases} \tag{38}$$

where

$$\tau_m = \frac{f_{\max} - f_{avg}}{\ell n(p_{m1}/p_{m2})}$$

f_m is the fitness value of the individual that would undergo mutation operation. k_m, p_{m1} and p_{m2} are the mutation coefficients. p_{m1} and p_{m2} are the constants between 0 and 1, and $p_{m1} > p_{m2}$. m is the mutation amplitude coefficient.

As cited above, the adaptive quantity which would vary with dispersion degree is added to the first term at the right side in Eq. (38). The second adaptive quantity which would vary with the fitness is added to the second term. The individual would be assigned a larger mutation rate p_{m1} when its fitness is worse than average (i.e. $f_m < f_{avg}$). If the fitness of the individual is better than average (i.e. $f_m \geqslant f_{avg}$), this individual would be assigned a smaller mutation rate which is exponentially decreased with the fitness beyond the average. In Eq. (38) we can observe that the mutation rate becomes smaller when the fitness value approaches the maximal fitness. When the fitness is equal to the maximal fitness, the mutation rate is p_{m2} rather than 0. The individual with the maximal fitness is uncertain of the global optimal solution. By using the adaptive mutation rate in Eq. (38), the fine individuals also have the chance to undergo the mutation operation, so that they would not get stuck at a local optimum.

4. Simulation results and discussions

Applying the proposed methodology in the real engineering optimization design, the procedures are briefly outlined as follows:

(1) Collect the weather database hourly
- wind speed,
- solar irradiation, and
- ambient temperature.

(2) Collect the load database hourly
- load power demand on an hourly basis.

(3) Input the wind generator data
- power-speed curve,
- installation height, and
- cost.

(4) Input the photovoltaic array data
- short circuit current, open circuit voltage, the maximum power current, the maximum power voltage, the short circuit current temperature coefficient, the open circuit voltage temperature coefficient, and
- cost.

(5) Input the battery data
- terminal voltages – state of charge curve in the charge state,
- terminal voltages – state of charge curve in the discharge state,

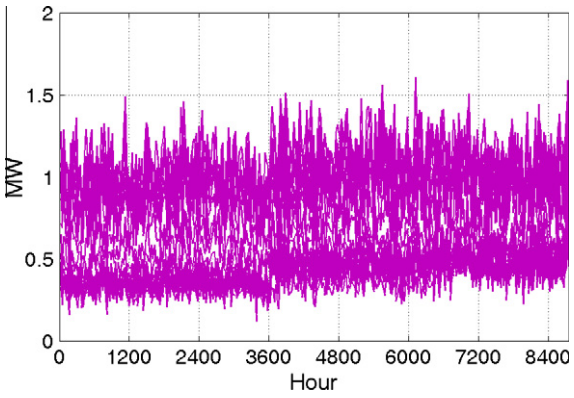

Fig. 6. Load power demand distribution during year 2011.

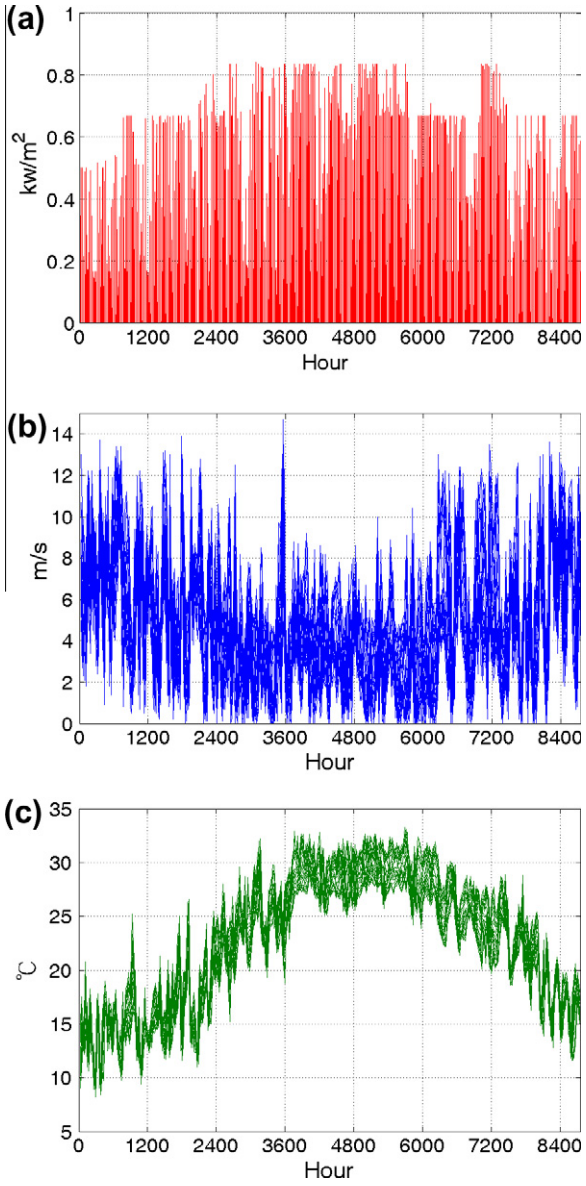

Fig. 7. Hourly (a) solar irradiance, (b) wind speed and (c) temperature distributions over year 2011 in Wuchi.

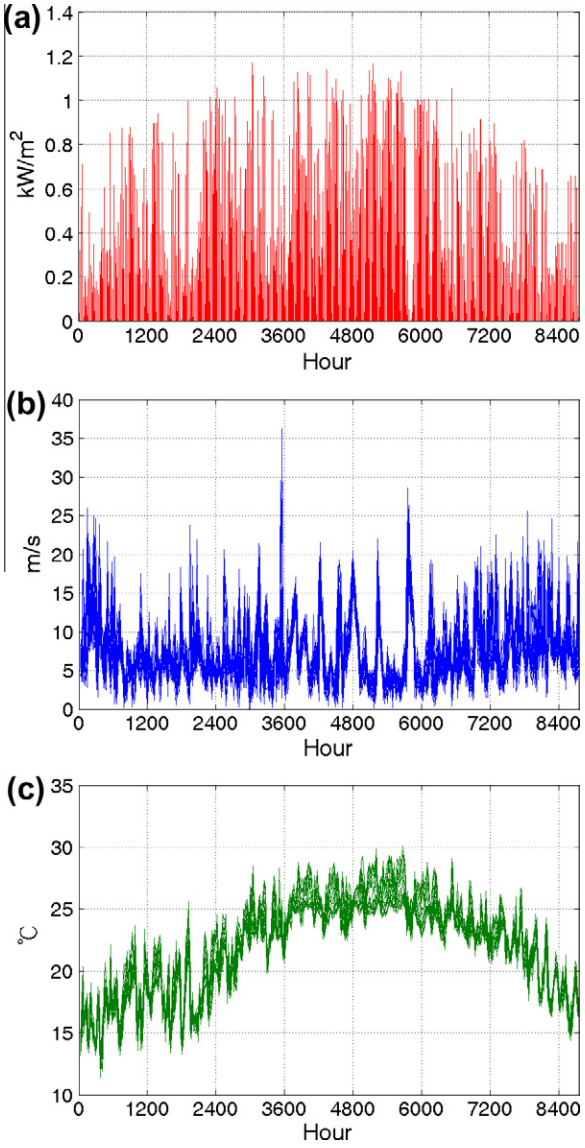

Fig. 8. Hourly (a) solar irradiance, (b) wind speed and (c) temperature distributions over year 2011 in the Orchid Island.

- internal resistor, self-discharge rate, charge/discharge efficiency, and
- cost.

(6) Input diesel engine data
- diesel engine cost, and
- fuel cost.

As such, the evaluation of weather effect on the power generation performance is truly affected by the number of days that weather observations are taken. Accordingly, a full year of weather variation and the power load demand observation is taken into account while the power capacity is optimized with a higher computational load.

The proposed methodology may equally well be applied to any other consumer and all potential types of wind generator, photovoltaic array and battery storage, in order to estimate the optimum

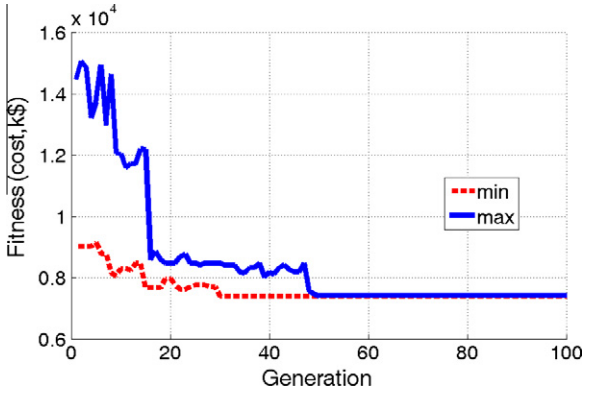

Fig. 9. Convergence curve of the adaptive genetic algorithm.

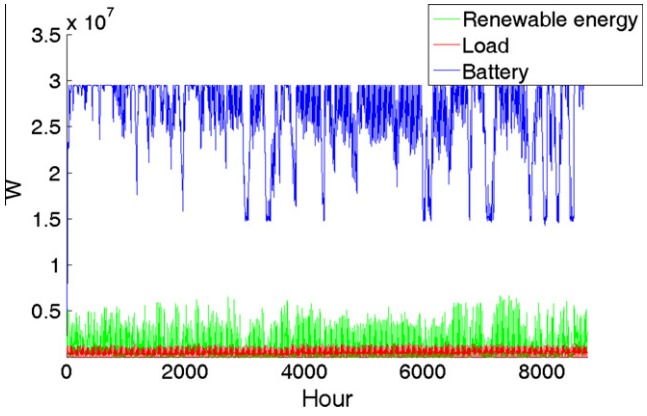

Fig. 10. Energy supply/demand distribution during year 2011.

hybrid system capacity that guarantees long-term energy autonomy. The characteristics of components are commercially available based on the technique datasheet provided from manufactures.

4.1. Example Analysis

As a design example, a load demand distribution over one full year 2011 requested by a machinery plant is presented in Fig. 6. Wuchi at Latitude 24°15′10″N and Longitude 120°31′57″E in the Taiwan and the offshore Orchid Island at Latitude 22°01′24″N and Longitude 121°33′26″E are chosen as two installation sites for an investigation into the weather effect on the optimization design.

Demonstrated in Figs. 7 and 8 are the hourly solar irradiance, wind speed and temperature detected in the full year 2011 at Wuchi and the Orchid Island, respectively. The annually average solar irradiances are 3.52 and 3.2 kW/m^2, wind speeds are 4.79 and 7.215 m/s, and temperatures are 22.52 and 21.86 °C in Wuchi and the Orchid Island, respectively.

Tabulated in Table 2 are the respective initial installation prices of power units.

The fitness function in an AGA is defined as the total initial installation cost, namely a minimized objective function as expressed in Eq. (30). A succession of constraints imposed on the

Table 2
Initial installation cost.

Equipment	600 kW wind generator	10 kW PV array	900AH battery bank	608 kW diesel generator
Cost (K$)	1200	34	10	79

Table 3
Optimization results with four WG models Enercon E40, Dewind D4-48, Nordex N43 and Vestas V42 (LOLP = 0.05, discharge depth = 30%).

Site	Wuchi				Orchid Island			
WG type	Enercon E40	Dewind D4-48	Nordex N43	Vestas V42	Enercon E40	Dewind D4-48	Nordex N43	Vestas V42
Wind generator	5	14	12	20	16	5	9	6
PV array	701	377	525	292	31	172	163	145
Battery bank	546	563	403	522	457	490	265	830
Total installation cost (K$)	35373	35327	36359	39227	24903	16827	19071	20509
Fuel cost (K$)	1.85	2.95	3.88	1.66	11.63	7.75	9.97	14.58

Table 4
Optimization results affected by the value of LOLP (WG model Dewind D4-48, discharge depth = 30%).

Site	Wuchi				Orchid Island			
LOLP constraint	0.05	0.1	0.15	0.2	0.05	0.1	0.15	0.2
Wind generator	14	7	16	14	5	7	7	5
PV array	377	464	131	233	172	134	36	63
Battery bank	563	499	432	218	490	130	124	144
Total installation cost (K$)	35327	29245	28053	26981	16827	14335	10943	9661
Fuel cost (K$)	2.95	21.78	64.60	79.74	7.75	38.03	113.15	120.57
CO_2 emission (ton)	5.74	42.33	125.55	154.97	15.07	73.9	219.9	234.24

Table 5
Optimization results affected by the discharge depth (WG model Dewind D4-48, discharge depth = 50%).

Site	Wuchi				Orchid Island			
LOLP constraint	0.05	0.1	0.15	0.2	0.05	0.1	0.15	0.2
Wind generator	8	3	2	2	6	3	3	4
PV array	489	482	383	397	121	122	114	62
Battery bank	329	279	347	199	369	299	151	49
Total installation cost (K$)	29595	22857	18971	17967	15083	10817	9065	7477
Fuel cost (K$)	20.49	57.04	105.77	136.97	23.63	79.56	131.80	166.31
CO_2 emission (ton)	39.82	110.84	205.55	266.17	45.92	154.6	256.13	323.2

system reliability is LOLP = 0.05, 0.1, 0.15 and 0.2, namely 438, 879, 1314 and 1752 h of load loss over 8760 h a year. The effect of LOLP on the installation cost can be seen through optimization. Exhibited in Fig. 9 is a plot of fitness (cost) against generation through an AGA convergence process at a specific case, from which it is seen that all the maximum and minimum fitness of individuals among an entire population converge toward a minimum value, i.e. the optimization solution that is wanted. Energy supply/demand distribution during the full year is shown in Fig. 10.

4.2. Effect analysis of WG power curves and installation sites

Tabulated in Table 3 are the optimization results with WGs in various models installed in Wuchi and the Orchid Island under the constraint LOLP = 0.5 at a battery discharge depth of 30%. The Dewind D4-48 is the one reaching the minimum total installation cost. This is due to the fact that, Dewind D4-48 is the one with the lowest cut-in and rated wind speeds compared with the other three as can be seen from the power curves in Fig. 2, meaning that it is of the highest generation efficiency for a given wind speed.

As tabulated in Table 2, the installation cost is on the order of 20 K$/KW for a wind turbine generator, while it is 3.4 K$/KW for a photovoltaic array. In Figs. 7 and 8, a point worthy of mention is that there is more abundant solar energy but less wind source in Wuchi than there is in the Orchid Island. Hence, as tabulated in Table 3, when meeting identical power load demand at two installation sites, it requires a larger number of photovoltaic arrays to offset a shortage of wind power in Wuchi. In a brief conclusion, the installation cost is found higher in Wuchi than in the Orchid Island for identical load demand.

4.3. Effect analysis of LOLP and battery discharge depth

Tabulated in Table 4 are the LOLP results by use of Dewind D4-48 WGs at a discharge depth of 30%. It is noted that the total installation cost decreases with LOLP and loss of load hour (LOLH), but increases with the system reliability. In other words, LOLH is a key factor to consider in determination of an acceptable LOLP.

With the same WGs as those in Table 4, optimization results are tabulated in Table 5 with a discharge depth up to 50%. An elevated discharge depth is found to save the initial installation cost as intended, but may lead to a shortened life cycle of a battery, that is, an increased maintenance cost in the long run.

A tremendous use of fossil fuels is known to be the major cause of CO_2 emission, a key issue to deal with in the global warming fact. According to a technical report [25], a MAN B&W 10K60MC diesel generator produces 590 g/KWh of CO_2, through which the total amount of CO_2 emission can be evaluated. As tabulated in Tables 4 and 5, while a higher capacity of renewable energy sources is found to increase the installation cost, it reduces the amount of CO_2 emission and become more environmentally friendly as a whole.

5. Conclusions

In this work, a methodology is presented to optimize the installation capacity of a stand-alone hybrid generation system. Accordingly, given a system configuration as well as an operation control strategy, a capacity optimization model is built in consideration of system reliability and cost. Subsequently, a full year of electricity generation contributed by wind generators and photovoltaic arrays

is estimated according to a long term weather database collecting the wind speed, temperature, solar irradiation, and so forth, all on an hourly basis. On top of that, an adaptive genetic algorithm is applied to a system match design for the solutions of capacity optimizations among individual system components. In the end, the optimization results are made at two distinct installation sites with this proposed methodology for comparison purpose.

Highly affected by seasons, a power load demand distribution demonstrates a significant influence on the capacity optimization result. For instance, the amount of electricity consumed in summertime is expected to be higher than the rest of a year. A neither stable nor uniform distribution of a renewable energy sources over an installation site will give rise to an elevated cost. The capacity and the discharge depth of a battery play a role in the dispatch of entire generation system. Hence, a more efficient use of renewable energy sources can be achieved in case a battery with high discharge depth is available. Since the cost of wind power generation is lower than that of solar power, the total installation cost can be reduced in windy areas, while meeting the power load demand. Optimization results are also related to specified LOLH, a quantity determined by a tradeoff between the electricity reliability and the system cost according to clients' demand.

Acknowledgment

The research was supported by the National Science Council of the Republic of China, under Grant No. NSC 101-ET-E-167-003-ET.

References

[1] Bekele G, Palm B. Feasibility study for a standalone solar–wind-based hybrid energy system for application in Ethiopia. Appl Energy 2010;87:487–95.
[2] Kalantar M, Mousavi G. Dynamic behavior of a stand-alone hybrid power generation system of wind turbine, microturbine, solar array and battery storage. Appl Energy 2010;87:3051–64.
[3] Khatod DK, Pant V, Sharma J. Analytical approach for well-being assessment of small autonomous power systems with solar and wind energy sources. IEEE Trans Energy Convers 2010;25:535–45.
[4] Chong WT, Naghavi MS, Poh SC, Mahlia TMI, Pan KC. Techno-economic analysis of a wind-solar hybrid renewable energy system with rainwater collection feature for urban high-rise application. Appl Energy 2011;88:4067–77.
[5] Tascikaraoglu A, Uzunoglu M, Vural B. The assessment of the contribution of short-term wind power predictions to the efficiency of stand-alone hybrid systems. Appl Energy 2012;94:156–65.
[6] Goel PK, Singh B, Murthy SS, Kishore N. Isolated wind–hydro hybrid system using cage generators and battery storage. IEEE Trans Ind Electron 2011;58:1141–53.
[7] Silva SB, Oliveira MAG, Severino MM. Sizing and optimization of hybrid photovoltaic, fuel cell and battery system. IEEE Lat A Trans 2011;9:817–22.
[8] Ekren O, Ekren BY, Ozerdem B. Break-even analysis and size optimization of a PV/wind hybrid energy conversion system with battery storage – a case study. Appl Energy 2009;86:1043–54.
[9] Ekren BY, Ekren O. Simulation based size optimization of a PV/wind hybrid energy conversion system with battery storage under various load and auxiliary energy conditions. Appl Energy 2009;86:1387–94.
[10] Ekren O, Ekren BY. Size optimization of a PV/wind hybrid energy conversion system with battery storage using simulated annealing. Appl Energy 2010;87:592–8.
[11] Zhou W, Lou CZ, Li ZS, Lu L, Yang HX. Current status of research on optimum sizing of stand-alone hybrid solar-wind power generation systems. Appl Energy 2010;87:380–9.
[12] Yang HX, Zhou W, Lou CZ. Optimal design and techno-economic analysis of a hybrid solar-wind power generation system. Appl Energy 2009;86:163–9.
[13] Saheb-Koussa D, Haddadi M, Belhamel M. Economic and technical study of a hybrid system (wind-photovoltaic-diesel) for rural electrification in Algeria. Appl Energy 2009;86:1024–30.
[14] Shrestha GB, Goel L. A study on optimal sizing of stand-alone photovoltaic stations. IEEE Trans Energy Convers 1998;13:373–8.
[15] Maghraby HAM, Shwehdi MH, Al-Bassam GK. Probabilistic assessment of photovoltaic generation systems. IEEE Trans Power Syst 2002;17:205–8.
[16] Kellog WD, Nehir MH, Venkataramanan G, Gerez V. Generation unit sizing and cost analysis for stand-alone wind, photovoltaic, and hybrid wind/PV systems. IEEE Trans Energy Convers 1998;13:70–5.
[17] Koutroulis E, Kolokotsa D, Potirakis A, Kalaitzakis K. Methodology for optimal sizing of stand-alone photovoltaic/wind-generator systems using genetic algorithms. Sol Energy 2006;80:1072–88.
[18] Chen HC. Optimal fuzzy PID controller design based on adaptive genetic algorithms. Dyn Contin Discrete Impuls Syst 2008;15:168–73.
[19] Khan MJ, Iqbal MT. Dynamic modeling and simulation of a small wind-fuel cell hybrid energy system. Renew Energy 2005;3:421–39.
[20] Nelson B, Nehrir MH, Wang C. Unit sizing analysis of stand-alone hybrid wind/PV/fuel cell power systems. Renew Energy 2006;10:1641–56.
[21] Chen HC, Qiu JC, Liu CH. Dynamic modeling and simulation of renewable energy based hybrid power systems. In: Proc. of third international conference on electric utility deregulation and restructuring and power technologies; 2008, p. O29.12-1–O29.12-7.
[22] Manwell JF, McGowan JG. A lead acid battery storage model for hybrid energy systems. Sol Energy 1993;50:399–405.
[23] Zbigniew Michalewicz. Genetic algorithms + data structures = evolution programs. 3rd Revised and Extended ed. New York: Springer; 2012.
[24] Green RC, Wang Z, Wang LF, Alam M, Singhy C. Evaluation of loss of load probability for power systems using intelligent search based state space pruning. In: Proc. of 11th IEEE international conference on probabilistic methods applied to power systems; 2010, p. 14–17.
[25] MAN B&W. Emission control of two-stroke low-speed diesel engines. MAN B&W Technical Paper; 1997.